



Open Access

## ORIGINAL ARTICLE

Sperm Biology

# Prokineticin 2 overexpression induces spermatocyte apoptosis in varicocele in rats

Ying Li<sup>1,\*</sup>, Ting Zhou<sup>2,\*</sup>, Yu-Fang Su<sup>1</sup>, Zhi-Yong Hu<sup>1</sup>, Jia-Jing Wei<sup>1</sup>, Wei Wang<sup>1</sup>, Chun-Yan Liu<sup>1</sup>, Kai Zhao<sup>1</sup>, Hui-Ping Zhang<sup>1</sup>

Varicocele is one of the most important causes of male infertility, as this condition leads to a decline in sperm quality. It is generally believed that the presence of varicocele induces an increase in reactive oxygen species levels, leading to oxidative stress and sperm apoptosis; however, the specific pathogenic mechanisms affecting spermatogenesis remain elusive. Prokineticin 2 (PK2), a secretory protein, is associated with multiple biological processes, including cell migration, proliferation, and apoptosis. In the testis, PK2 is expressed in spermatocytes under normal physiological conditions. To investigate the role of PK2 in varicocele, a rat varicocele model was established to locate and quantify the expression of PK2 and its receptor, prokineticin receptor 1 (PKR1), by immunohistochemistry and quantitative real-time PCR assays (qPCR). Moreover, H<sub>2</sub>O<sub>2</sub> was applied to mimic the oxidative stress state of varicocele through coculturing with a spermatocyte-derived cell line (GC-2) *in vitro*, and the apoptosis rate was detected by flow cytometry. Here, we illustrated that the expression levels of PK2 and PKR1 were upregulated in the spermatocytes of the rat model. Administration of H<sub>2</sub>O<sub>2</sub> stimulated the overexpression of PK2 in GC-2. Transfection of recombinant pCMV-HA-PK2 into GC-2 cells promoted apoptosis by upregulating cleaved-caspase-3, caspase-8, and B cell lymphoma 2-associated X; downregulating B cell lymphoma 2; and promoting the accumulation of intracellular calcium. Overall, we revealed that the varicocele-induced oxidative stress stimulated the overexpression of PK2, leading to apoptosis of spermatocytes. Our study provides new insight into the mechanisms underlying oxidative stress-associated male infertility and suggests a novel therapeutic target for male infertility.

Asian Journal of Andrology (2020) 22, 500–506; doi: 10.4103/aja.aja\_109\_19; published online: 19 November 2019

**Keywords:** apoptosis; oxidative stress; prokineticin 2; varicocele

## INTRODUCTION

Infertility affects 10%–15% of couples worldwide. Varicocele is one of the most important causes of male infertility and is associated with approximately 40% of cases.<sup>1</sup> Varicocele is characterized by the abnormal dilation and tortuosity of spermatic veins, which results from obstruction of spermatic venous drainage or blood reflux.<sup>2</sup> It is generally believed that the presence of varicocele induces an increase of reactive oxygen species (ROS), leading to oxidative stress, sperm chromosomal abnormalities, and sperm apoptosis;<sup>3</sup> however, the specific pathogenic mechanisms affecting spermatogenesis remain elusive. Common treatments for varicocele include open scrotal or inguinal varicocelectomy, microsurgical varicocelectomy, laparoscopic varicocelectomy, and embolization.<sup>2</sup> However, a controversy exists over whether these operations improve the sperm quality and conception rate.<sup>4,5</sup> Thus, further investigation into the mechanisms of pathogenicity is necessary for the treatment of varicocele-induced male infertility.

Prokineticin 2 (PK2), a small secretory protein of 14 kD, is constitutively bound to G-protein-coupled receptor prokineticin receptor 1 (PKR1), mediating multiple biological processes, including cell migration, proliferation, and apoptosis.<sup>6,7</sup> However, the role of PK2 in the apoptotic process is controversial. Overexpression of PK2

or PKR1 has been shown to induce vessel-like formations in cardiac endothelial cells, as well as in cardiomyocytes, with serine/threonine kinase (AKT) activation that protects cardiomyocytes against oxidative stress.<sup>8</sup> In contrast,  $\beta$ -amyloid-induced apoptosis in cortical neurons is associated with an upregulation of PK2, which is nullified by the PK2 antagonist PC-1, indicating that PK2 is a key mediator in the  $\beta$ -amyloid-induced neuronal damage.<sup>9</sup> However, the associated investigation in the reproductive system remains limited.

Under normal physiological conditions, PK2 is highly expressed in the testis and is primarily located in the primary spermatocytes. In PK2 knockout mice, gonadotropin-releasing hormone (GnRH) secretory dysfunction results in sexual development and fertility impairment in males, represented by small seminiferous tubules with lumens that lack haploid spermatocytes and spermatids.<sup>10</sup> In our previous studies, PK2 is upregulated in the rat model of lipopolysaccharide (LPS)-induced orchitis<sup>11</sup> and experimental autoimmune orchitis,<sup>12</sup> indicating that PK2 is involved in testicular inflammation. Pro-inflammatory cytokines, such as interleukin-1 $\alpha$  (IL-1 $\alpha$ ), IL-6, and tumor necrosis factor- $\alpha$  (TNF- $\alpha$ ), are significantly increased in varicocele, suggesting that a chronic testicular inflammation occurs.<sup>13</sup> Moreover, hypoxia-ischemia and reactive oxygen species (ROS) stimulate the upregulation of PK2

<sup>1</sup>Family Planning Research Institute/Reproductive Medicine Center, Tongji Medical College, Huazhong University of Science and Technology, Wuhan 430030, China;

<sup>2</sup>Department of Gynecology and Obstetrics, Union Hospital, Tongji Medical College, Huazhong University of Science and Technology, Wuhan 430030, China.

\*These authors contributed equally to this work.

Correspondence: Dr. HP Zhang (zhpmed@126.com)

Received: 18 December 2018; Accepted: 25 July 2019

in primary cortical cultures,<sup>14</sup> and varicocele is also correlated with hypoxia and oxidative stress.

Considering the important role of PK2 in testicular inflammation and oxidative stress, we considered whether PK2 was a critical node of sperm apoptosis in varicocele. Our previous study proved that PK2 mRNA was upregulated in a rat model of varicocele;<sup>15</sup> however, a more detailed investigation of the underlying mechanism is warranted. In this study, we demonstrate that the expression of PK2 and its receptor PKR1 is upregulated in spermatocytes in a varicocele rat model. Moreover, oxidative stress stimulated the overexpression of PK2 in a spermatocyte-derived cell line, GC-2, *in vitro*. The overexpression of PK2 in GC-2 cells promoted apoptosis by upregulating cleaved-caspase-3, caspase-8, and B cell lymphoma 2-associated X (Bax); downregulating B cell lymphoma 2 (Bcl-2); and promoting the accumulation of intracellular calcium. Thus, apoptosis induced by the PK2/PKR1 pathway in spermatocytes may serve as a potential target for reducing the varicocele-induced impairment of sperm quality.

## MATERIALS AND METHODS

### Animals

Twenty adult male Wistar rats (180–200 g) were purchased from the Hubei Provincial Center for Disease Control and Prevention (Wuhan, China). The animals were maintained at 22°C with a 12 h/12 h light/dark cycle and fed with standard food pellets and water *ad libitum*. All animal experiments were performed in strict accordance with the approved guidelines from the Institutional Animal Care and Use Committee of Tongji Medical College, Huazhong University of Science and Technology (Wuhan, China). The study was approved by the Ethics Committee of Huazhong University of Science and Technology.

### Establishment of a rat varicocele model

Twenty male Wistar rats were randomly divided into two groups, namely, the sham control and varicocele groups. After being anesthetized with 10 g tribromoethanol (Sinopharm Chemical Reagent Co., Shanghai, China) and 10 ml tert-pentyl alcohol (Sinopharm Chemical Reagent Co.) diluted to 2% in distilled water, a 2 cm incision was made in the hypogastrium of the rats. The left renal vein was isolated at its junction with the inferior vena cava. A blunt dissection channel was made between the inside of the left renal vein and the outside of the inferior vena cava; then, a 4-0 silk suture was placed to narrow the left renal vein to half of its original diameter. The same surgical procedure without the ligation was performed in the sham control group. Successful modeling criteria included (i) diameter of the spermatic vein >1 mm, and (ii) no difference in size between the left and right kidneys. The rats were killed 8 weeks after the operation.

### TUNEL assay

DNA fragmentation of the testis was assessed with terminal deoxynucleotidyl transferase dUTP nick end labeling (TUNEL) assay using the TUNEL Apoptosis Detection Kit (FITC; Yeasen, Shanghai, China) following the manufacturer's instructions. The testicular sections were incubated with FITC-12-dUTP Labeling Mix and recombinant TdT enzyme in equilibration buffer for 60 min at 37°C and protected from light. Labeled cryosections were detected by fluorescence microscopy (Olympus, Tokyo, Japan) at 520 nm.

### Measurement of SOD and MDA

The levels of testicular superoxide dismutase (SOD) in the varicocele and the sham operation groups were quantified with a Total Superoxide Dismutase Assay Kit with NBT (Beyotime, Shanghai, China) according to the manufacturer's instructions. Superoxide anion radicals generated

from xanthine and xanthine oxidase reduce NBT to blue formazan. Superoxide anion radicals are eliminated by SOD. The absorbance of blue formazan in each sample was detected using a multimode microplate reader (BioTek Synergy™ HTX, Winooski, VT, USA) at 450 nm.

Malondialdehyde (MDA) levels were determined by a Lipid Peroxidation MDA Assay Kit (Beyotime), which is based on the ability of MDA to react with thiobarbituric acid to generate a red product. The absorbance of each sample was determined by a multimode microplate reader (BioTek Synergy™ HTX) at 535 nm.

### Sperm analysis

The left cauda epididymitis was cut into pieces and incubated in 2 ml Ham's F10 medium (Jimei, Beijing, China) for 5 min at 37°C to allow the spermatozoa to swim out. One drop of sperm suspension (10 µl) was placed on a Neubauer hemocytometer and then covered with a 24 mm × 24 mm cover slip, and the cells were assessed with a microscope (Olympus) at ×400 magnification. In one chamber, the number of spermatozoa in the central grid and corner grids was assessed and the average was calculated. The percentage of motile spermatozoa was evaluated according to the WHO (2010) recommendations.<sup>16</sup> Motility was expressed as the percentage of motile spermatozoa of two hundred cells assessed. Spermatozoa of Grade A (fast progressive) and Grade B (slow progressive) motility were identified.

### Western blot

The testicular tissue was lysed on ice with radioimmunoprecipitation assay lysis buffer (Cwbio, Taizhou, China). Subsequently, 20–40 µg of protein was electrophoresed on an 8%–12% (*w/v*) sodium dodecyl sulfate-polyacrylamide gel gradient and transferred to a nitrocellulose membrane. The membranes were blocked with 5% (*w/v*) nonfat milk for 1 h in Tris-buffered saline (TBS) and subsequently incubated with the following primary antibodies: rabbit anti-PK2 antibody (1:200, Abcam, Cambridge, MA, USA), rabbit anti-cleaved-caspase-3 antibody (1:1000, Cell Signaling Technology [CST], Boston, MA, USA), rabbit anti-caspase-8 antibody (1:1000, CST), rabbit anti-Bax antibody (1:1000, CST), rabbit anti-Bcl-2 antibody (1:1000, CST), and mouse anti-β-actin antibody (1:500, Boster, Wuhan, China). Immunoreactive bands were detected using electrochemiluminescence (ECL; Pierce, Waltham, MA, USA).

### Quantitative real-time PCR assays (qPCR)

The TRIzol reagent (Invitrogen, Carlsbad, CA, USA) was used to extract total RNA from the rat testes. Reverse transcription was performed using a PrimeScript™ RT Reagent Kit (Takara, Kusatsu, Japan) according to the manufacturer's instructions. The 20 µl qPCR reaction included 2 µl cDNA, 0.8 µl forward primers, 0.8 µl reverse primers (Table 1), and 10 µl SYBR Green qPCR MasterMix (Takara). The qPCR amplification procedure was performed in a thermocycler (Roche, Basel, Switzerland). Relative expression levels of the target

**Table 1: Quantitative polymerase chain reaction primer sequences**

Gene	Type	Primer sequences (5'–3')	Length (bp)
PK2	Forward	CAAGGACTCTCAGTGTGGA	128
	Reverse	AAAATGGAACCTTCCGAGTC	
PKR1	Forward	TGGGCGAGAATACCACAA	182
	Reverse	GCCATGCCAATGACAATC	
β-actin	Forward	GATGAGATTGGCATGGCTTT	101
	Reverse	CACCTTCACCGTTCCAGTTT	

PK2: prokineticin 2; PKR1: prokineticin receptor 1



genes were normalized with those of the controls with the  $2^{-\Delta\Delta Ct}$  method.

### Immunohistochemistry

The rat was perfuse-fixed with 300–350 ml 4% formaldehyde solution (Servicebio, Wuhan, China) after 200 ml normal saline via a perfusion needle in the left ventricle of the heart for 45 min. Then, the testis was removed and immersion fixed in the same fixative for 4–6 h. Testicular sections were stained with hematoxylin–eosin (H and E; Solarbio, Beijing, China) to determine the histological changes. To assess the location of PK2 and PKR1 in the rat testes, the sections were subjected to antigen retrieval by heating in citric acid buffer (0.018 mol l<sup>-1</sup> citric acid monohydrate and 0.082 mol l<sup>-1</sup> trisodium citrate dihydrate [Sinopharm Chemical Reagent Co.], pH 6.0) at 95°C for 15 min. After natural cooling, the sections were incubated in PBS containing 3% (v/v) H<sub>2</sub>O<sub>2</sub> for 20 min to inhibit endogenous peroxidase activity. Then, the testicular sections were blocked with 2.5% (w/v) nonfat milk for 10 min and incubated with the primary antibodies: rabbit anti-PK2 antibody (1:200, Abcam) and rabbit anti-PKR1 antibody (1:500, Alomone, Jerusalem, Israel) overnight at 4°C. The EnVision™ Detection Kit (Dako, Copenhagen, Denmark), based on the diaminobenzidine (DAB) working principle, was used to detect the expression of PK2 and PKR1. The signal was detected in an optical microscope (Olympus).

### Immunofluorescence

The GC-2 cells were seeded on a cover slip and fixed with cooled 4% (w/v) formaldehyde at 4°C for 20 min. After blocking with 5% (v/v) normal goat serum (Beyotime) at room temperature for 1 h, the cells were incubated with the rabbit anti-PK2 antibody (1:200, Abcam) or rabbit anti-PKR1 antibody (1:500, Alomone) at 4°C overnight. After the cells were washed twice with PBS, the secondary antibody, goat anti-rabbit IgG H&L (FITC; 1:500, Abcam), was incubated with the cells at room temperature for 1 h. The cell nuclei were stained with 4',6-diamidino-2-phenylindole (DAPI; biofroxx, Einhausen, Germany). The fluorescence intensity was detected with a fluorescence microscope (Olympus).

### Cell proliferation

Cell proliferation was measured using the Cell Counting Kit 8 (CCK8; Dojindo, Tokyo, Japan). GC-2 cells at a density of  $1 \times 10^4$  ml<sup>-1</sup> (100 µl per well) were seeded in a 96-well plate. After the cell density reached 80% of the well, the culture medium was replaced with serum-free Dulbecco's modified eagle medium (DMEM; Gibco, Carlsbad, CA, USA) to starve the cells for 12 h. Then, the cells were processed at various concentrations of H<sub>2</sub>O<sub>2</sub> (0, 200, 400, and 600 µmol l<sup>-1</sup>) or cocultured with different concentrations of plasmids (empty plasmid control pCMV-HA, 4 µg and 8 µg pCMV-HA-PK2 expression plasmid). After 24 h, the fluid was removed, and 10% (w/v) CCK8 in DMEM was added. The cells were maintained at 37°C for 2 h. The absorbance of each sample was determined at 450 nm in a multimode microplate reader (BioTek Synergy™ HTX). The optical density (OD) was used to calculate cell proliferation as follows: cell proliferation (%) = (mean OD of treated cells/mean OD of untreated cells) × 100%.

### Construction and transfection of pCMV-HA-PK2 expression plasmid

A double restriction enzyme (*Hind* III and *Xho* I; Fermentas, Waltham, MA, USA) was used to cut the PK2 DNA fragment and mammalian expression vehicle pCMV-HA, respectively. Then, the purified target fragment of the PK2 gene was directionally recombined with the pCMV-HA vehicle by the T4 DNA ligase system (Fermentas). The recombinant plasmid was transformed into Top10 Chemically

Competent *E. coli* (Invitrogen) by shorten heat shock; then, their mixture was mixed with liquid Luria-Bertani culture medium to amplify *E. coli*. The amplified bacterial suspension was coated on Luria-Bertani culture media containing 50 µg ml<sup>-1</sup> ampicillin. After incubation overnight at 37°C, the monoclonal strain was extracted and would be amplified after correct gene sequencing. Plasmid extraction procedure was instructed from the Plasmid Miniprep Kit (Tsingke, Beijing, China). The recombinant plasmid was transiently transfected into GC-2 cells with Lipofectamine 2000 (Invitrogen). In brief, the transfection complex, including the optimized concentrations of plasmid and Lipofectamine 2000, was transferred to the 80% confluent GC-2 cells for 6 h, and then those cells were washed and further cultured in DMEM for 42 h.

### Flow cytometric analysis

Cell apoptosis was detected by the FITC Annexin V Apoptosis Detection Kit (BD, Franklin Lakes, NJ, USA) following the manufacturer's protocol. Cell suspensions containing  $1 \times 10^5$  cells were transferred to a FACS tube. After being washed twice with PBS, the cells were resuspended in 200 µl binding buffer (0.1 mol l<sup>-1</sup> HEPES/NaOH [pH 7.4], 1.4 mol l<sup>-1</sup> NaCl, and 25 mmol l<sup>-1</sup> CaCl<sub>2</sub>) with 5 µl Annexin V for 15 min, avoiding the light. Then, 5 µl of propidium iodide (PI) was added to the suspension. The rate of apoptosis of the cells was assessed immediately in a flow cytometer (BD), and the data were analyzed with FlowJo software version X (BD).

### Measurement of intracellular calcium concentration

To measure the concentration of intracellular calcium, GC-2 cells were loaded for 60 min with 2.5 µmol l<sup>-1</sup> Fura-3 AM (Beyotime) at 37°C. After being washed, the cells were incubated with Fura-3 AM for more 20 min to ensure the complete conversion to Fura-3. The accumulated Fura-3 in cells combines with Ca<sup>2+</sup>, which is excited at 488 nm and was detected in a fluorescence microscope. The fluorescence intensity represents the concentration of intracellular calcium.

### Statistical analyses

The statistical analyses were conducted with the SPSS 18.0 (IBM, New York, NY, USA) and GraphPad Prism software 5.0 (GraphPad, San Diego, CA, USA). The data are presented as the mean ± standard deviation (s.d.). An unpaired *t*-test was used to analyze the differences between the two groups. One-way ANOVA was used to analyze the intergroup differences among multiple groups. *P* < 0.05 was considered statistically significant.

## RESULTS

### Testicular histology and sperm quality in varicocele

After 8 weeks, the varicocele group demonstrated abnormal dilation of spermatic veins (**Figure 1a**). In the histological analysis, the testes of the varicocele group were characterized by a thinner spermatogenic epithelium and the vacuolization of the germinal epithelium. The proportion of tubules that presented vacuolization in the varicocele was higher than that in the control samples (75.0% ± 4.0% vs 19.7% ± 4.4%) (**Figure 1b**). The result of the TUNEL assay indicated that the number of positive testicular cells (those with DNA damage) was higher in the varicocele group than that in the control group (**Figure 1c**). Furthermore, in the varicocele group, the concentration of SOD was decreased (*P* = 0.011; **Figure 1d** and **Supplementary Table 1**), and MDA was increased (*P* = 0.009; **Figure 1e** and **Supplementary Table 1**) compared with the control group. Varicocele was shown to reduce the progressive motility of epididymal spermatozoa (*P* = 0.041), but not the sperm number (*P* = 0.317) (**Figure 1f, 1g** and **Supplementary Table 1**).

### Expression of PK2 and PKR1 in varicocele

PK2 was mainly expressed in primary spermatocytes, with weaker signals observed in spermatogonial cells and spermatids. PKR1 also exhibited diffuse expression in primary spermatocytes (Figure 2a). For quantitative evaluation, PK2 and PKR1 expression was detected by qPCR and Western blot. The mRNA of PK2 and PKR1 was upregulated in the varicocele group compared with the control group ( $P = 0.008$  and  $P = 0.003$ , respectively) (Figure 2b and Supplementary Table 1). At the protein level, an increase in PK2 was observed in the varicocele group (Figure 2c).

### PK2 expression and oxidative stress in GC-2 cells

To explore the role of PK2/PKR1 signaling in varicocele, the spermatocyte cell line GC-2 was used for *in vitro* experiments. GC-2 cells exhibit characteristics similar to those of primary spermatocytes in terms of PK2 and PKR1 expression (Figure 3a). Subsequently, various concentrations of  $H_2O_2$  were added to the GC-2 culture medium to mimic the oxidative stress state of varicocele.  $H_2O_2$  reduced the number of viable cells in culture in a dose-dependent manner (0 vs 200  $\mu\text{mol l}^{-1}$ :  $P = 0.029$ ; 0 vs 400  $\mu\text{mol l}^{-1}$ :  $P = 0.0001$ ; and 0 vs 600  $\mu\text{mol l}^{-1}$ :  $P = 0.0001$ ; Figure 3b and Supplementary Table 2). After  $H_2O_2$  treatment, the mRNA expression of PK2 was upregulated in GC-2 cells compared with the control cells (0 vs 200  $\mu\text{mol l}^{-1}$ :  $P =$

0.066 and 0 vs 400  $\mu\text{mol l}^{-1}$ :  $P = 0.009$ ; Figure 3c and Supplementary Table 2). The protein expression of PK2 was increased after  $H_2O_2$  treatment (Figure 3d).

### Overexpression of PK2 and GC-2 apoptosis

To further investigate the potential mechanism by which PK2 regulated apoptosis, a PK2 plasmid was transfected into GC-2. In the PK2-overexpressed group, an increase in the rate of apoptosis was detected by flow cytometry with Annexin IV/PI staining (Figure 4a). Cell viability was decreased in the transfected groups compared with the control group with an empty vector plasmid (0 vs 4  $\mu\text{g}$ :  $P = 0.006$  and 0 vs 8  $\mu\text{g}$ :  $P = 0.003$ ; Figure 4b and Supplementary Table 3). Upregulation of the apoptosis-associated proteins such as cleaved-caspase-3, caspase-8, and Bax and downregulation of Bcl-2 were observed in PK2-overexpressed cells by Western blot (Figure 4c). The supernatants of the PK2 plasmid cultures promoted intracellular  $Ca^{2+}$  levels in GC-2 cells (Figure 4d).

### DISCUSSION

Several studies have suggested that oxidative stress is a significant cause of sperm quality reduction, which results from the imbalance between ROS and antioxidants.<sup>17</sup> ROS in sperm-free seminal fluid has been shown to be significantly increased in infertile men with varicocele compared with that in fertile healthy men, and antioxidants such as SOD, catalase, and glutathione peroxidase have been shown to be decreased. Seminal MDA, an indicator of lipid peroxidation induced by ROS, is related to decreased sperm concentration, sperm motility, as well as normal sperm forms in man.<sup>18,19</sup> Our results in rats are consistent with previous data in rats on the vacuolization of the seminiferous epithelium and reduction in progressive sperm motility, accompanied

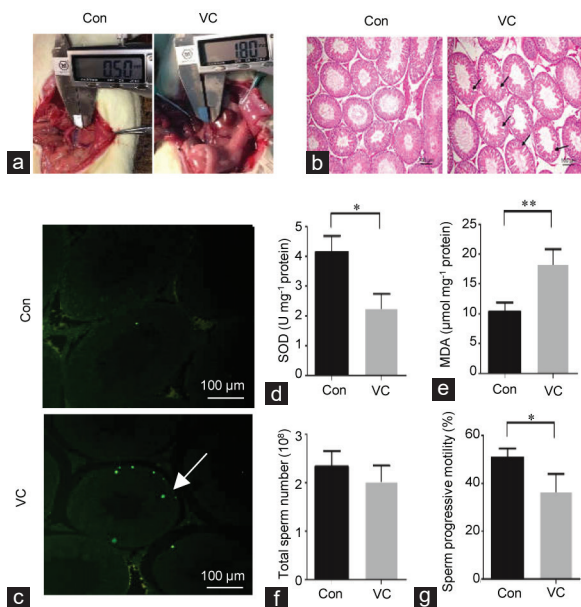


**Figure 1:** Testicular histology and sperm quality in varicocele. (a) Diameter of the spermatic vein was assessed after 8 weeks in the control group and the varicocele group. (b) Testicular tissue sections stained with hematoxylin and eosin reveal the histopathological changes. Spermatogenic cells are arranged neatly and orderly in a concentric distribution in controls. The deleterious effects (mainly vacuolization of the germinal epithelium as indicated by arrows) are observed in the varicocele group. The scale bar represents 100  $\mu\text{m}$ . (c) The TUNEL assay was performed on the control and varicocele to detect DNA strand breakage in testicular cells. Positive green cells of the TUNEL (+) test are indicated with arrows. The scale bars represent 100  $\mu\text{m}$ . (d) The concentration of SOD was measured in the control and varicocele testes. (e) The concentration of MDA was measured in control and varicocele testes. In the cauda epididymidis, (f) the total sperm number and (g) progressive motility were assessed in control and varicocele. Sample sizes are  $n = 3$  from different rats for each group. Each treatment group compared with the control group,  $*P < 0.05$ ,  $**P < 0.01$  (*t*-test). SOD: superoxide dismutase; TUNEL: terminal deoxynucleotidyl transferase dUTP nick end labeling; MDA: malondialdehyde; Con: control group; VC: varicocele group.

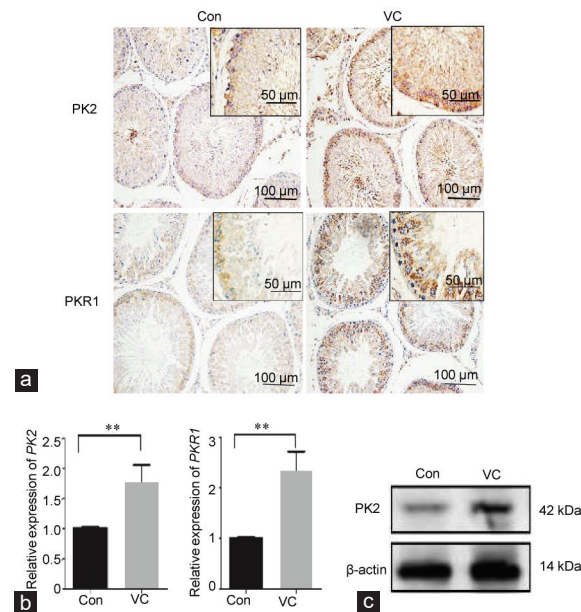


**Figure 2:** Expression of PK2 and PKR1 in varicocele. (a) Immunohistochemical staining of PK2 and PKR1 in the rat testes. Control testes display a weak PK2 signal. The immunoreactivity of PK2 is increased in the VC group. Control testes display a weak PKR1 signal. The immunoreactivity of PKR1 is increased in the VC group. The scale bar represents 50  $\mu\text{m}$  or 100  $\mu\text{m}$ . (b) Alteration of PK2 and PKR1 mRNA in the testes was analyzed by qPCR. (c) The protein level of PK2 was determined by Western blot. Sample sizes are  $n = 3$  for each group. Each treatment group was compared with the control group,  $**P < 0.01$  (*t*-test). PK2: prokineticin 2; PKR1: prokineticin receptor 1; qPCR: quantitative real-time PCR assays; Con: control group; VC: varicocele.

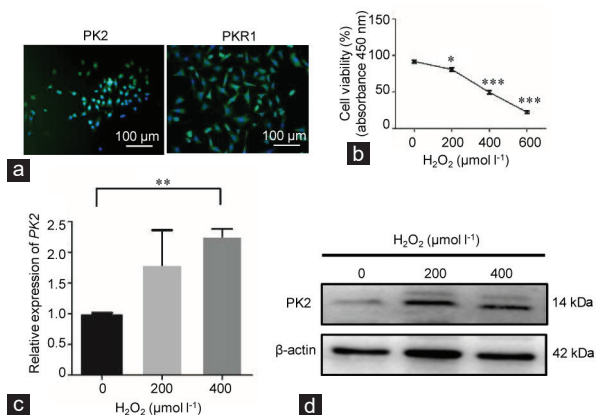


**Figure 3:** PK2 expression and oxidative stress in GC-2 cells. GC-2 cells were cocultured with various concentrations of H<sub>2</sub>O<sub>2</sub> (0, 200, 400, and 600 μmol l<sup>-1</sup>) for 6 h. (a) The basal expression levels of PK2 and PKR1 in GC-2 cells were determined by immunofluorescence. The scale bars represent 100 μm. (b) The viability of GC-2 cells in the different groups was determined by CCK8 assay. (c) Alterations in the mRNA expression of PK2 in GC-2 cells in the different groups were determined by qPCR. (d) Alteration of the protein expression of PK2 in GC-2 cells in the different groups was analyzed by Western blot. All experiments were replicated in three independent experiments from different cell samples. Each treatment group was compared with the control group, \**P* < 0.05, \*\**P* < 0.01, \*\*\**P* < 0.001 (one-way ANOVA). PK2: prokineticin 2; PKR1: prokineticin receptor 1; qPCR: quantitative real-time PCR assays; ANOVA: analysis of variance.

by decreased levels of SOD and increased activity of MDA in testicular tissue, indicating that oxidative stress occurred in varicocele.<sup>20,21</sup>

Aerobic metabolism of spermatozoa evokes the production of seminal ROS, which potentially damages the sperm plasma membrane as well as the core nuclear chromatin.<sup>22</sup> Leukocytes act as another major source of seminal ROS.<sup>23</sup> Compared with healthy men, varicocele-associated subfertility and infertility is associated with an increase in seminal leukocytes.<sup>24</sup> The accumulation of polyunsaturated fatty acids in the sperm plasma membrane and a low antioxidant capacity make sperm vulnerable to ROS attack.<sup>25</sup> On the other hand, H<sub>2</sub>O<sub>2</sub> has previously been applied to mimic oxidative stress conditions in primary cortical cultures.<sup>14</sup> H<sub>2</sub>O<sub>2</sub> induces oxidative stress in GC-2 cells by suppressing the expression levels of antioxidant enzymes and triggering reduction of the viability of GC-2 cells.<sup>26</sup> Similar results were also observed in our study. Our results demonstrated that oxidative stress reduced the viability of GC-2 cells; however, the detailed mechanism is unclear.

PK2, a pro-inflammatory secretory protein, has been shown to elevate the inflammatory response by recruiting the infiltration of neutrophils and macrophages in inflamed tissues and upregulating pro-inflammatory cytokines.<sup>6,27,28</sup> In the mammalian reproductive system, PK2 is primarily expressed in the prostate and testis and is particularly highly expressed in spermatocytes. Moreover, after being injected with the PK2 protein through the rete testis of adult rats to establish the PK2 overexpression model, the testes presented inflammatory histological changes with an increased infiltration of interstitial cells and disintegration of the seminiferous epithelium.<sup>12</sup> Previous research has suggested that varicocele is an inflammation-activated state that is associated with increased levels of inflammatory markers, such as seminal epithelial neutrophil activating peptide-78 and IL-1β.<sup>29</sup> In the present study, we established that the expression levels of PK2 and its receptor PKR1 were increased in varicocele at the protein level, suggesting that the PK2/PKR1 signaling pathway

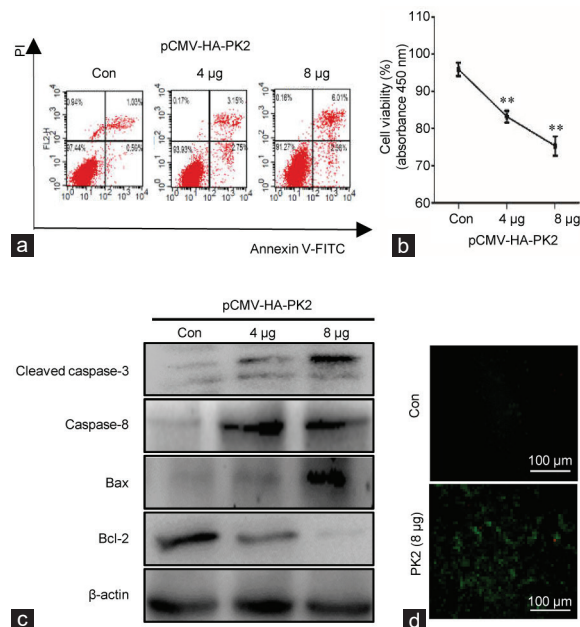


**Figure 4:** Overexpression of PK2 and GC-2 apoptosis. GC-2 cells were either transfected with various concentrations of the pCMV-HA-PK2 plasmid (4 μg and 8 μg), or empty vector plasmid for 48 h as a control. (a) The apoptosis rate was quantified by flow cytometry of GC-2 cells labeled with Annexin V-FITC and PI. (b) Cell viability in the different groups with various concentrations of plasmid was determined by CCK8 assay. (c) The cell lysates were analyzed by Western blotting with antibodies against cleaved-caspase-3, caspase-8, Bax, and Bcl-2. (d) The concentrations of intracellular calcium of GC-2 cells were determined by immunofluorescence. The scale bars represent 100 μm. All experiments were replicated in three independent experiments from different cell samples. Con: the cells were transfected with an empty vector. Each treatment group was compared with the control group, \*\**P* < 0.01 (one-way ANOVA). PK2: prokineticin 2; Bax: B cell lymphoma 2-associated X; Bcl-2: B cell lymphoma 2; ANOVA: analysis of variance.

mediated the development of inflammation-related varicocele. Because of the difficulty of primary spermatocyte culture and intervention *in vitro*, we chose a more stable cell line, as there is no rat spermatocyte line at present. It has been reported that the N-terminal region of PK2 has a hexapeptide sequence called “AVITGA” that is conserved in all species. The AVITGA sequence is essential for the biological activities and the binding to PK2 receptors. Considering the high conservation of PK2 in different species, we chose GC-2 for *in vitro* experiments.<sup>30</sup> Furthermore, for the first time, we demonstrated that PK2 and PKR1 are expressed in GC-2 cells, indicating that these cells could potentially be used as a model to study the PK2 signaling pathway *in vitro*.

Emerging information suggests that there may exist a close relation between PK2 and oxidative stress. In our previous research, inducible nitric oxide synthase (iNOS), an indicator of the degree of oxidative stress, was upregulated in rat spermatocytes after PK2 overexpressed in testis, suggesting that PK2 may impair the testis by inducing oxidative stress.<sup>12</sup> *In vitro* stimulation with H<sub>2</sub>O<sub>2</sub> upregulates mRNA expression of PK2 in primary cortical cultures.<sup>14</sup> In our study, H<sub>2</sub>O<sub>2</sub> was administered to mimic the oxidative stress state of varicocele *in vitro*, and both the mRNA and protein expression of PK2 were also increased in GC-2 cells after the oxidant challenge, suggesting that PK2 is positively correlated with oxidative stress in germ cells. Given that leukocytes are the primary generator of ROS, we infer that an abnormal infiltration of inflammatory cells in varicocele elicits a microenvironment of oxidative stress, which is caused, in part, by the overexpression of PK2.

Studies that focus on the relationship between PK2 and apoptosis are limited and controversial. PK2 is known to attenuate H<sub>2</sub>O<sub>2</sub>-induced apoptosis in cardiomyocytes,<sup>8</sup> while in cortical neurons, upregulation of PK2 promotes the amyloid- $\beta$  peptide-induced neuronal damage.<sup>9</sup> In an attempt to confirm the role of PK2 in germ cell apoptosis, the pCMV-HA-PK2 plasmid was transfected into GC-2 cells to upregulate the expression of PK2. The rate of apoptosis was increased in the overexpressed group by the activation of apoptosis-associated proteins, such as cleaved-caspase-3, caspase-8, and Bax. It has become evident that PK2 has varying effects on apoptosis, depending on the cell type. PK2 promotes the survival of cardiomyocytes and angiogenesis through antagonizing oxidative stress, whereas it triggers neuron and germ cell apoptosis through the activation of oxidative stress. We infer that the role of PK2 in the apoptotic process in a cell is dependent on whether it is positively correlated with oxidative stress. In spermatocytes, the mutually reinforcing relationship between PK2 and oxidative stress triggers apoptosis signaling cascades.

PK2 action is known to elevate intracellular Ca<sup>2+</sup> levels through voltage-gated Ca<sup>2+</sup> channels in subfornical organ neurons.<sup>31</sup> This increase has the potential to disturb Ca<sup>2+</sup> homeostasis and evoke apoptosis through oxidative stress and endoplasmic reticulum stress activation.<sup>32</sup> In our study, the overexpression of PK2 led to accumulation of intracellular Ca<sup>2+</sup> in GC-2 cells, suggesting that PK2 participates in the endoplasmic reticulum stress pathway to induce apoptosis. On the other hand, PK2 and its receptor transduce G-protein signals, suggesting that they are involved in multiple intracellular signaling cascades, such as mitogen-activated protein kinase (MAPK), extracellular-regulated MAP kinase (ERK1/2), and AKT.<sup>33,34</sup> The question of whether AKT, ERK1/2, or other pathways participate in PK2-induced apoptosis warrants further investigation.

In our research, PK2 and PKR1 were upregulated in spermatocytes in a rat model of varicocele. The administration of H<sub>2</sub>O<sub>2</sub> to mimic the oxidative stress status of varicocele *in vitro* induced an increase of PK2 and PKR1. The overexpression of PK2 triggered GC-2 cell apoptosis and Ca<sup>2+</sup> influx; however, the specific underlying mechanism remains unclear. Collectively, PK2 played an important role in the pro-apoptotic process of oxidative stress in varicocele. Our study provides a new viewpoint to reveal the mechanisms underlying oxidative stress-associated male infertility. Moreover, these data highlight that PK2 is a potential modulatory biomarker in varicocele, which may help in the development of a new therapeutic target for male infertility.

#### AUTHOR CONTRIBUTIONS

YL and HPZ designed research studies, analyzed data, and drafted the manuscript. TZ conducted rat model establishment, Western blot, qPCR, and immunohistochemistry. YFS conducted rat model establishment, cell culture, and immunofluorescence. ZYH conducted flow cytometry and semen analysis. JJW and WW conducted construction and transfection of pCMV-HA-PK2 expression plasmid. CYL and KZ provided intellectual input into planning of experiments and contributed to the writing of the manuscript. All authors read and approved the final manuscript.

#### COMPETING INTERESTS

All authors declared no competing interests.

#### ACKNOWLEDGMENTS

This work was supported by the National Natural Science Foundation of China (Grant No. 81871148, No. 81701539 and No. 81571496).

Supplementary Information is linked to the online version of the paper on the *Asian Journal of Andrology* website.

#### REFERENCES

- Baigorri BF, Dixon RG. Varicocele: a review. *Semin Intervent Radiol* 2016; 33: 170–6.
- Choi WS, Kim SW. Current issues in varicocele management: a review. *World J Mens Health* 2013; 31: 12–20.
- Ni K, Steger K, Yang H, Wang H, Hu K, *et al*. A comprehensive investigation of sperm DNA damage and oxidative stress injury in infertile patients with subclinical, normozoospermic, and astheno/oligozoospermic clinical varicocele. *Andrology* 2016; 4: 816–24.
- McGarry P, Alrabeeh K, Jarvi K, Zini A. Is varicocelectomy beneficial in men previously deemed subfertile but with normal semen parameters based on the new guidelines? A retrospective study. *Urology* 2015; 85: 357–62.
- Dun RL, Yao M, Yang L, Cui XJ, Mao JM, *et al*. Traditional chinese herb combined with surgery versus surgery for varicocele infertility: a systematic review and meta-analysis. *Evid Based Complement Alternat Med* 2015; 2015: 689056.
- Negri L, Ferrara N. The prokineticins: neuromodulators and mediators of inflammation and myeloid cell-dependent angiogenesis. *Physiol Rev* 2018; 98: 1055–82.
- Sasaki S, Baba T, Muranaka H, Tanabe Y, Takahashi C, *et al*. Involvement of prokineticin 2-expressing neutrophil infiltration in 5-fluorouracil-induced aggravation of breast cancer metastasis to lung. *Mol Cancer Ther* 2018; 17: 1515–25.
- Urayama K, Guilini C, Messaddeq N, Hu K, Steenman M, *et al*. The prokineticin receptor-1 (GPR73) promotes cardiomyocyte survival and angiogenesis. *FASEB J* 2007; 21: 2980–93.
- Caioli S, Severini C, Ciotti T, Florenzano F, Pimpinella D, *et al*. Prokineticin system modulation as a new target to counteract the amyloid beta toxicity induced by glutamatergic alterations in an *in vitro* model of Alzheimer's disease. *Neuropharmacology* 2017; 116: 82–97.
- Pitteloud N, Zhang C, Pignatelli D, Li JD, Raivio T, *et al*. Loss-of-function mutation in the prokineticin 2 gene causes Kallmann syndrome and normosmic idiopathic hypogonadotropic hypogonadism. *Proc Natl Acad Sci U S A* 2007; 104: 17447–52.
- Chen B, Yu L, Wang J, Li C, Zhao K, *et al*. Involvement of prokineticin 2 and prokineticin receptor 1 in lipopolysaccharide-induced testitis in rats. *Inflammation* 2016; 39: 534–42.
- Li Y, Wang J, Yu L, Zhao K, Chen B, *et al*. Effects of prokineticin 2 on testicular inflammation in rats. *Am J Reprod Immunol* 2018; 79: e12843.
- Oh YS, Jo NH, Park JK, Gye MC. Changes in inflammatory cytokines accompany deregulation of claudin-11, resulting in inter-sertoli tight junctions in varicocele rat testes. *J Urol* 2016; 196: 1303–12.
- Cheng MY, Lee AG, Culbertson C, Sun G, Talati RK, *et al*. Prokineticin 2 is an endangering mediator of cerebral ischemic injury. *Proc Natl Acad Sci U S A* 2012; 109: 5475–80.
- Tu LH, Yu LL, Xiong CL, Zhang HP. Potential role of prokineticin 2 in experimental varicocele-induced rat testes. *Urology* 2012; 80: 952.e15–9.
- World Health Organization. Laboratory Manual for the Examination and Processing of Human Semen. 5<sup>th</sup> ed. Geneva: World Health Organization; 2010. p32–6.
- Minutoli L, Puzzolo D, Rinaldi M, Irrera N, Marini H, *et al*. ROS-mediated NLRP3 inflammasome activation in brain, heart, kidney, and testis ischemia/reperfusion injury. *Oxid Med Cell Longev* 2016; 2016: 2183026.
- Mostafa T, Anis T, Imam H, El-Nashar AR, Osman IA. Seminal reactive oxygen species-antioxidant relationship in fertile males with and without varicocele. *Andrologia* 2009; 41: 125–9.
- Wang H, Lv Y, Hu K, Feng T, Jin Y, *et al*. Seminal plasma leptin and spermatozoon apoptosis in patients with varicocele and leucocytospermia. *Andrologia* 2015; 47: 655–61.
- Asadi N, Kheradmand A, Gholami M, Moradi FH. Effect of ghrelin on the biochemical and histopathology parameters and spermatogenesis cycle following experimental varicocele in rat. *Andrologia* 2018; 50: e13106.
- Taghizadeh L, Eidi A, Mortazavi P, Rohani AH. Effect of selenium on testicular damage induced by varicocele in adult male Wistar rats. *J Trace Elem Med Biol* 2017; 44: 177–85.
- Ramya T, Misro MM, Sinha D, Nandan D. Sperm function and seminal oxidative stress as tools to identify sperm pathologies in infertile men. *Fertil Steril* 2010; 93: 297–300.
- Lobascio AM, De Felici M, Anibaldi M, Greco P, Minasi MG, *et al*. Involvement of seminal leukocytes, reactive oxygen species, and sperm mitochondrial membrane potential in the DNA damage of the human spermatozoa. *Andrology* 2015; 3: 265–70.
- Tortolero I, Duarte Ojeda JM, Pamplona Casamayor M, Alvarez González E, Arata-Bellabarba G, *et al*. The effect of seminal leukocytes on semen quality in subfertile males with and without varicocele. *Arch Esp Urol* 2004; 57: 921–8.
- Walczak-Jedrzejowska R, Wolski JK, Slowikowska-Hilczek J. The role of oxidative stress and antioxidants in male fertility. *Cent European J Urol* 2013; 66: 60–7.
- Kopalli SR, Cha KM, Jeong MS, Lee SH, Sung JH, *et al*. Pectinase-treated Panax ginseng ameliorates hydrogen peroxide-induced oxidative stress in GC-2 sperm



- cells and modulates testicular gene expression in aged rats. *J Ginseng Res* 2016; 40: 185–95.
- 27 Giannini E, Lattanzi R, Nicotra A, Campese AF, Grazioli P, *et al*. The chemokine Bv8/prokineticin 2 is up-regulated in inflammatory granulocytes and modulates inflammatory pain. *Proc Natl Acad Sci U S A* 2009; 106: 14646–51.
- 28 Martucci C, Franchi S, Giannini E, Tian H, Melchiorri P, *et al*. Bv8, the amphibian homologue of the mammalian prokineticins, induces a proinflammatory phenotype of mouse macrophages. *Br J Pharmacol* 2006; 147: 225–34.
- 29 Hassanin AM, Ahmed HH, Kaddah AN. A global view of the pathophysiology of varicocele. *Andrology* 2018; 6: 654–61.
- 30 Kaser A, Winklmayr M, Lepperdinger G, Kreil G. The AVIT protein family. Secreted cysteine-rich vertebrate proteins with diverse functions. *EMBO Rep* 2003; 4: 469–73.
- 31 Fry M, Cottrell GT, Ferguson AV. Prokineticin 2 influences subfornical organ neurons through regulation of MAP kinase and the modulation of sodium channels. *Am J Physiol Regul Integr Comp Physiol* 2008; 295: R848–56.
- 32 Yin L, Dai Y, Cui Z, Jiang X, Liu W, *et al*. The regulation of cellular apoptosis by the ROS-triggered PERK/EIF2 $\alpha$ /chop pathway plays a vital role in bisphenol A-induced male reproductive toxicity. *Toxicol Appl Pharmacol* 2017; 314: 98–108.
- 33 Lin DC, Bullock CM, Ehlert FJ, Chen JL, Tian H, *et al*. Identification and molecular characterization of two closely related G protein-coupled receptors activated by prokineticins/endocrine gland vascular endothelial growth factor. *J Biol Chem* 2002; 277: 19276–80.
- 34 Chen J, Kuei C, Sutton S, Wilson S, Yu J, *et al*. Identification and pharmacological characterization of prokineticin 2 beta as a selective ligand for prokineticin receptor 1. *Mol Pharmacol* 2005; 67: 2070–6.

---

This is an open access journal, and articles are distributed under the terms of the Creative Commons Attribution-NonCommercial-ShareAlike 4.0 License, which allows others to remix, tweak, and build upon the work non-commercially, as long as appropriate credit is given and the new creations are licensed under the identical terms.

©The Author(s)(2019)

**Supplementary Table 1: Statistical analysis of *in vivo* experiment**

	<i>Control (n=3)</i>	<i>Varicocele (n=3)</i>	<i>Figure</i>
SOD (U/mg protein)	4.1±0.4	2.3±0.4	1
MDA (μmol/mg protein)	10.3±1.2	18.3±2.1	1
Sperm total number/10 <sup>6</sup>	2.3±0.3	2.0±0.3	1
Progressive sperm motility (%)	50.7±3.1	36.7±5.9	1
Relative expression of PK2	1.0	1.8±0.2	2
Relative expression of PKR1	1.0	2.4±0.3	3

PK2: prokineticin 2; PKR1: prokineticin receptor 1; SOD: superoxide dismutase; MDA: malondialdehyde

**Supplementary Table 2: Statistical analysis of Figure 3**

	<i>0 μM</i>	<i>200 μM</i>	<i>400 μM</i>	<i>600 μM</i>
Relative expression of PK2	1	1.8±0.5	2.3±0.1	–
Cells viability (%)	91.8±2.8	81.1±3.6	49.7±3.0	22.6±1.9

PK2: prokineticin 2

**Supplementary Table 3: Statistical analysis of Figure 4**

	<i>0</i>	<i>4 μg</i>	<i>8 μg</i>
Cells viability (%)	95.9±2.5	83.2±2.2	75.4±3.7